

Development of Motorcycle Engine Starting System Simulation Considering Air-Fuel Ratio Control

Yoshihito Itou Daiki Itou Minoru Iida

当論文は、SAE 2017-32-0045 / JSAE 20179045として、SETC2017(Small Engine Technology Conference)にて発表されたものです。

Reprinted with permission Copyright © 2017SAE Japan and Copyright © 2017SAE International.
(Further use or distribution is not permitted without permission from SAE.)

要旨

昨今、燃費向上や排出ガス削減の観点より、二輪車におけるアイドルストップシステムの採用が拡大している。アイドルストップ車両ではエンジン停止後の再始動が頻繁に行われるため、スロットル入力から発進までの時間短縮による発進時操作性の確保や、未燃炭化水素の排出低減のための始動時の速やかなエンジン回転上昇が従来に増して重要となっている。

そこで筆者らは、エンジン始動時の回転上昇における主要な因子である燃焼と空燃比との関係を実験的に明らかにしたうえで、始動時の吸気ポート内噴射燃料の蒸発モデルおよび低温環境を含む始動時のエンジン回転速度の変化を机上検討できる始動システムのシミュレーションを開発した。

さらに本手法は、空燃比制御を成立させるクランキング回転速度および速やかなエンジン回転上昇を実現するデコンプレッティングの検討が可能であることを異なる噴射系の適用例を通して示した。

Abstract

Recently the response of the engine speed at starting has more importance than ever for quick start satisfying rider's needs, as well as exhaust emissions. We have developed a simulation for studying engine and starter specifications, engine control algorithm and other engine control parameters. This system can be utilized to realize appropriate starting time by considering air-fuel ratio under various conditions.

This paper addresses what are taken account of in our method. Examples applying this to a conventional motorcycle engine are shown.

1

INTRODUCTION

In recent years, emphasis on fuel economy improvements has driven a trend toward increasing number of motorcycle models equipped with idling-stop system. In such systems, engine speed increase at startup^[1] is critical to reduce vehicle take-off time at engine restart^[2] and hydrocarbon emissions at startup^[3-4]. Since multiple elements, such as combustion, electrical components, control logic, and decompressors, affect the engine speed change, coordinated design that satisfies the conditions required for engine startup, has become increasingly challenging^[5].

In regard to securing engine speed increase at startup, the air-fuel ratio control necessary for generating

sufficient combustion torque is considered particularly important; however, if the motor cranking speed is increased to reduce the time from startup to vehicle take-off, the time from fuel injection to intake stroke completion also drops, leading to concerns that there may not be sufficient fuel vaporization in the inlet ports under low temperatures, resulting in insufficient cylinder fuel density and poor engine speed increase or ignition failure. Unfortunately, there are very few reported examples to simulate startability that include aspects such as air-fuel ratio control and electrical components. A lot of motorcycle engines equip mechanical decompressor in order to reduce the size and weight of the starter and battery. It is possible to reduce the drop in engine speed in the compression stroke by decreasing

pressure through retarding decompressor operation during cranking. However, this may lead to poor starting due to decrease amount of mixture in the cylinder available at the first combustion, which results in reduced engine speed increases at the first combustion.

In order to quantitatively understand the complex relation of each component, we have developed a simulator to predict engine behavior at start. Relation between engine speed increase at start and mixture air-fuel ratio has been also identified experimentally.

In this report we outline the simulator and discuss examples of improvements to starter motor control and decompressor specifications that make air-fuel ratio control enable.

2

REPRESENTATION OF COMBUSTION AT STARTUP

The following two points are given as the main requirements relating to fuel injection control at engine startup:

- 1) To supply sufficient fuel to control the cylinder air-fuel ratio at the appropriate level for generating sufficient combustion torque to prevent poor starting and achieve a reduction in startup time.
- 2) To reduce excess fuel injection in order to reduce hydrocarbons and prevent plug fouling.

The fuel vaporization rate depends on the injector position and direction of injection, as well as the spray characteristics and temperature of the gas in the intake port. In particular under cold conditions, the fuel vaporization rate drops significantly due to decline in gasoline vapor pressure. This makes it difficult to inject the amount of fuel necessary to achieve the appropriate air-fuel ratio in the cylinder until the end of the induction stroke at the first cycle. As a result, the air-fuel mixture density may become diluted, leading to insufficient engine speed increase, and poor starting.

If we then increase the motor cranking speed to shorten the startup time, the time taken from the commencement

of startup injection to the end of the intake stroke is reduced. This causes difficulties in supplying the required fuel into the cylinder, resulting in potential emission of unburned gas due to ignition failures or delay of engine speed increase caused by decrease in combustion torque.

From the above concerns, we have confirmed through experiments the relationship of fuel spray vaporization under low engine temperature conditions and cylinder air-fuel ratio to combustion torque generation. We have also tried to show importance on the relationship between fuel injection duration at startup (taking into account fuel injection specifications and cranking speed) and cylinder air-fuel mixture density, etc. for the purpose of determining system feasibility relating to fuel injection control at startup.

2-1. Method of experiments

The engine speed during the intake stroke of the first combustion cycle at startup is low, and therefore the volumetric efficiency is large and there is little residual burned gas in the cylinder, making this cycle similar to combustion at full load. Thanks to this, the resulting torque is large, and the engine, which has a small moment of inertia about the crankshaft axis, reaches engine speed close to its idling target. Accordingly, if we focus on the engine speed increase at startup, it seems that the combustion torque contribution of the first cycle is large compared with the cycles that follow. Thus, we have confirmed the exhaust gas equivalence ratio related to engine speed increase during first combustion cycle by changing the first injection duration.

We used an air-cooled two-valve single-cylinder research engine with displacement of 125[cm³] for the test. For the running conditions, we altered the ambient temperature, injection direction, injection timing, and injector type. The injection point was kept fixed when the injection direction was changed. The ISC (idle speed controller) valve opening was fixed at the calibration value at startup across the entire temperature range, and the throttle main valve was open assuming idling.

In order to estimate the equivalence ratio in the

cylinder, HFR500 and NDIR500 was used to measure the instantaneous THC, CO, and CO₂ in the exhaust port within a cycle (Fig. 1).

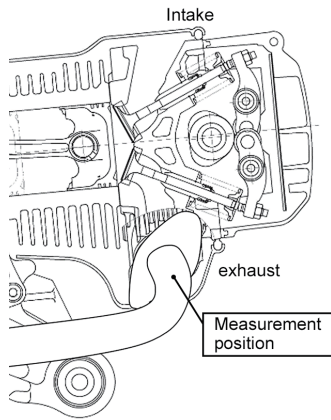


Fig.1 Measurement position of exhaust gas

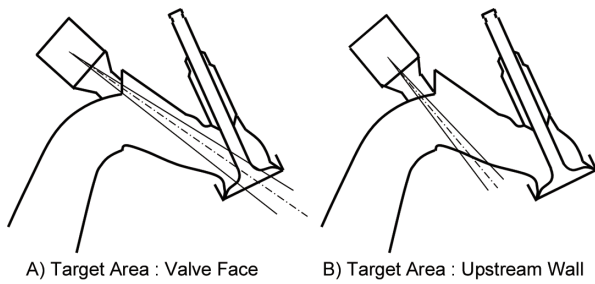


Fig.2 Overview of fuel injection

2-2. Result of experiments

The relationship between the injection duration and the engine speed increase at the first combustion is indicated in Figure 3. The vertical axis ΔNe represents the amount of increase in engine speed over the interval starting at the compression top dead center until 180 degrees of crank angle later (Fig. 4).

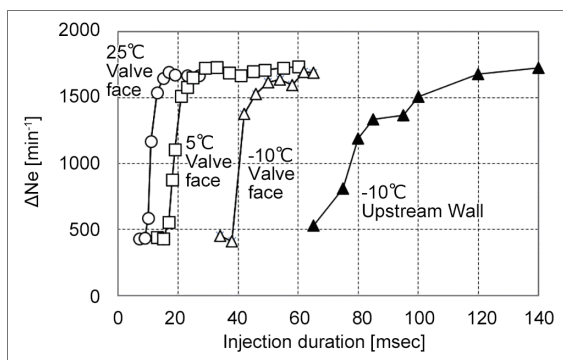


Fig.3 Relation between injection duration and ΔNe

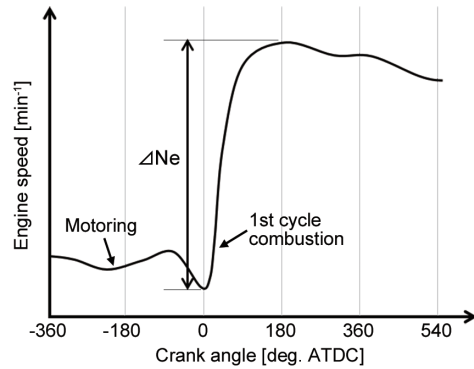


Fig.4 Definition of ΔNe

It was found that the injection duration for sufficient engine speed increase during the first combustion cycle was highly dependent on the engine temperature. Moreover, in case of the injection direction aiming at the upstream wall, significantly longer injection duration was needed than the cases aiming to the intake valve, so as to increase engine speed sufficiently.

The engine speed increase with respect to the equivalence ratio is indicated in Figure 5. The injector shown as “small SMD” in Figure 5 gives spray with small SMD (85 → 76 [μm]) and broader spray angle. (22.8 → 25.6 [deg])

In the range where the exhaust gas equivalence ratio was less than one, the engine speed increase rose as the exhaust gas equivalence ratio increased. In the range where the exhaust gas equivalence ratio was one or more, the engine speed increase barely changed despite increase in the exhaust gas equivalence ratio. At this point, injection direction, injection timing, injector type, and engine temperature caused little difference to the maximum of engine speed increase during the first combustion. We have concluded from these data that the engine speed increase during the first combustion depends only on the equivalence ratio in the cylinder under condition of fixed intake throttle. It can be also stated that the cylinder air-fuel ratio should be set to the stoichiometry in order to maximize the engine speed increase at the first combustion as well as to minimize excessively supplied fuel.

	Engine Temperature [degC]	Target Area	Injection Timing (SOI)	Injector Type	
○	A	25	Valve face	Intake	STD
□	B	5	Valve face	Intake	STD
△	C	5	Valve face	Intake	Small SMD
●	D	-10	Valve face	Intake	STD
■	E	-10	Valve face	Intake	Small SMD
▲	F	-10	Valve face	Compression	STD
◆	G	-10	Upstream Wall	Compression	STD

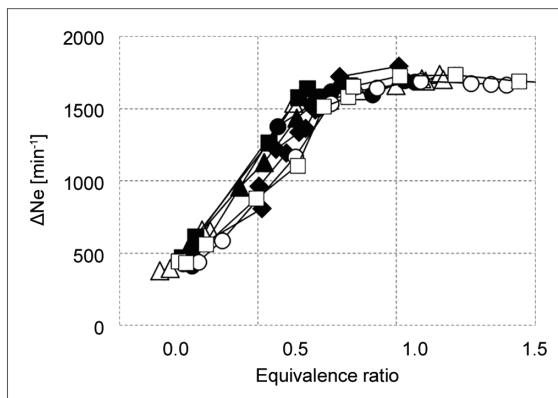


Fig.5 Relation between equivalence ratio and increase amount of engine speed

2-3. Fuel transportation model to calculate the cylinder equivalence ratio at first cycle

Based on the experimental results described in the previous section, in order to both maximize the engine speed increase at the first combustion cycle and reduce excess fuel injection duration at the same time, it was hypothesized that the injection duration should be set so that the mixture in the cylinder is stoichiometry.

The fuel spray vaporization and behavior at startup are modeled bearing in mind the time constraints when working on startup systems, the engine temperature range necessary for consideration, and the range of design specifications.

The amount of evaporation of drop flying in an intake port is calculated by using the equation (1).^[6]

$$\frac{dm_d}{dt} = -A_d Sh \frac{D_{AB}}{D_d} \rho_V \ln \frac{(1 - Y_{v,\infty})}{(1 - Y_{v,s})} \alpha \quad (1)$$

where, m_d is the mass of drop, A_d is the equivalent area of drop, Sh is Sherwood number, D_{AB} is the diffusion coefficient, D_d is the drop diameter, ρ_V is the density of

mixture, $Y_{v,\infty}$ is the fuel mass fraction of the atmosphere, $Y_{v,s}$ is the fuel mass fraction of drop surface, and α is an adjustment factor of evaporation.

It is necessary to know the flight distance of the fuel drop in order to calculate the flight time of the fuel drop. The flight distance is defined as from the injection point to the impingement point to the wall. For obtaining the above information, we use the three-dimensional shape of the intake port.

- The fuel spray vaporization during travel in the intake port is derived as follows from the vaporization behavior of a single drop (as described later):

- The air temperature, pressure, and density surrounding the drop are set as the average value in the intake port during the injection period.

- The drop temperature is set to equal the engine environment temperature, and it is postulated that this would not change while moving.

- For the fuel, data regarding the physical properties of the fuel consisting of the vapor pressure at different temperature etc. is set as the input value to enable simulation of the fuel vaporization rate based on the change in temperature.

- The overall spray vaporization rate is calculated by weighting the appearance frequency distribution of the drop with diameter.

The fuel droplets behavior are postulated as follows:

- Effect of air flow on drop velocity is neglected.

- The drop velocity changes by air drag force. Drop breakup is discounted.

- 100% of drops impinging on to the wall adhere

to the wall surface, and fuel vaporization from the liquid film on the wall is neglected.

- The initial velocity of the drop from the injector is calculated from the fuel pressure.
- Weighting according to the spray spatial density distribution obtained from the test rig is applied.

The injection timing which results in an equivalence ratio of 1 for the different injection directions (Fig.2) are estimated using the above methods, and the results compared to the experiment results are shown in Figure 6.

It is found that the injection duration which makes the cylinder equivalence ratio equal to the theoretical air-fuel ratio has been predicted to within 20% of that of the experiment result, with all engine temperature conditions. Moreover, it is also confirmed that this calculation model has good predictability regarding injection specifications which shorten the spray movement distance by orienting the injection direction towards the wall.

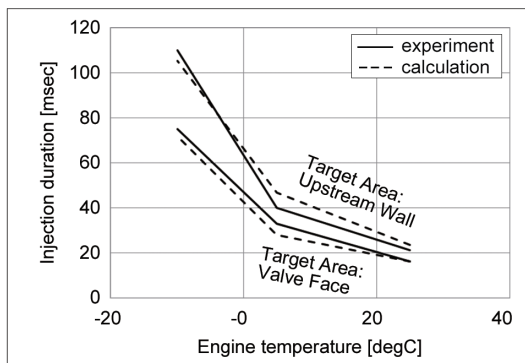


Fig.6 Relation between engine temperature and injection duration at stoichiometric air-fuel ratio

3 STARTUP SYSTEM SIMULATION

3-1. Simulation outline

A startup system simulation as shown in Figure 7 was developed including the fuel transport model introduced in the previous section. Modeling of the constituent elements other than the fuel transport model, including the motor, battery, motor control logic, and friction loss, will be described in the following section.

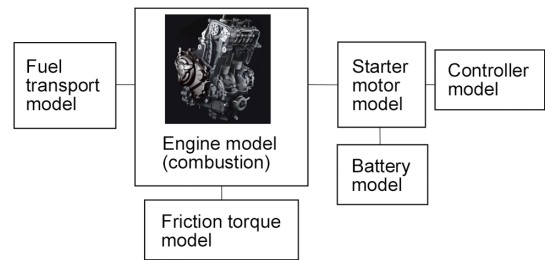


Fig.7 Overview of engine start system simulations

3-2. Modeling of each element

3-2-1. Starter motor

A DC brushless motor is used in this case. The motor control mode, battery voltage, and motor speed are inputted, and the motor torque and battery current are outputted. Furthermore, the energizing control method, rotation direction, and duty value are determined according to the motor control mode.

The motor torque and motor current are measured in advance on a stand-alone motor basis, and modeled as a map depending on the battery voltage and advance angle (Fig. 8).

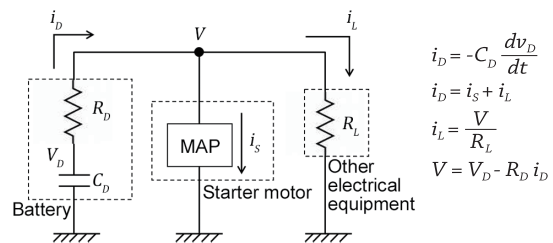


Fig.8 Model of electrical system

3-2-2. Battery

Battery capacity is estimated based on the voltage drop curve during high rate discharge measured on a stand-alone battery basis. A map to show battery capacity is conducted within the range used during engine start.

3-2-3. Motor control logic

Motor control logic is modeled using MATLAB/Simulink (Fig. 9). The motor control mode is outputted by inputting the engine crank angle, engine speed, and starter switch signal.

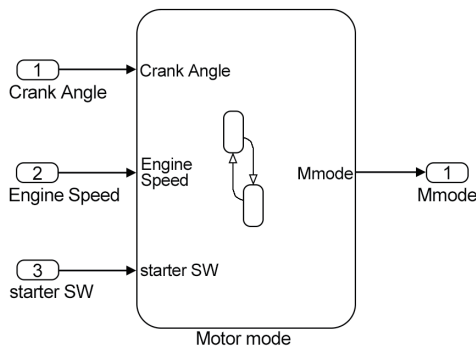


Fig.9 Motor controller model

3-2-4. Engine mechanical friction torque

Modeling has been conducted on an experimental basis for each part in the engine and auxiliary equipment, which was used to calculate the total engine friction loss value before executing the simulation, in turn provided to the system simulation as a map of friction loss with respect to engine speed changes and oil temperature.

Making the major engine specifications relating to friction loss into input values enables consideration of startability that takes into account changes in friction loss according to changes in specification.

4 APPLICATION EXAMPLES OF STARTUP SYSTEM SIMULATION

A startup system simulation was conducted incorporating the calculation model described before. The examples introduced here are feasibility study of the engine startup system with various engine specifications from the following perspectives.

1. Air-fuel ratio control feasibility
2. Startability

4-1. Consideration of air-fuel ratio control feasibility

The tolerance range of controllable cranking speed which makes the cylinder equivalence ratio equal to the theoretical air-fuel ratio during low-temperature startup was calculated.

Fig.10 depicts the range of the cranking rotational speed at which the air-fuel ratio control is established. Where, the value of the vertical axis is normalized with the upper

limit of cranking speed for air-fuel ratio control at -10 degrees C.

We can see that the cranking speed which generates sufficient combustion torque at the first combustion depends on the temperature: it becomes lower as the temperature decreases. As the spray traveling distance becomes shorter by changing in the injection direction, the upper limit of the engine speed at which the air-fuel ratio is controllable decreases.

In this way, it has been found that the cranking speed at which air-fuel ratio control at startup is feasible varies depending on the fuel injection position, direction, intake port shape layout, and injector specifications.

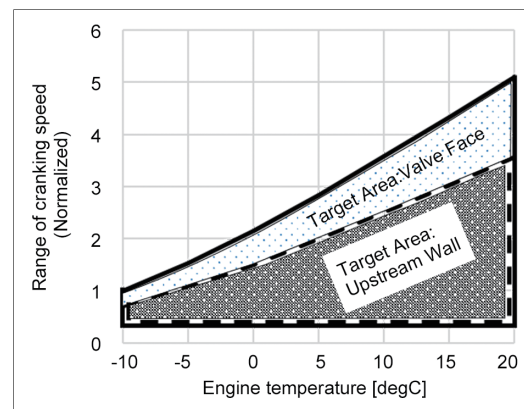


Fig.10 The range of the cranking rotational speed at which the air-fuel ratio control is established

4-2. Consideration of engine speed responsiveness at startup

The next phase of consideration involved securing engine speed increase at startup from the perspective of reducing take-off time at engine restart.

The characteristics of the engine speed change at startup (Fig. 11) are as follows:

- Because the test engine has a small moment of inertia about the crankshaft axis and is a single-cylinder unit, it has a big instantaneous drop in engine speed during the compression stroke (Fig. 11, A). Such large drop in instantaneous engine speed can cause failure in starting.

- In order to prevent too big drop of speed, decompressor is equipped usually for this type of engines. A problem may occur, when the decompressor reactivates during the compression stroke in the second combustion cycle (Fig. 11, B), due to the engine speed decrease after the engine speed increase in the first combustion cycle. If this happen, the decompressor may continue to activate and cause poor starting.

- Changing the decompressor timing changes the amount of fresh air in the cylinder used for combustion, enabling greater engine speed increase at first combustion and reduction in startup time.

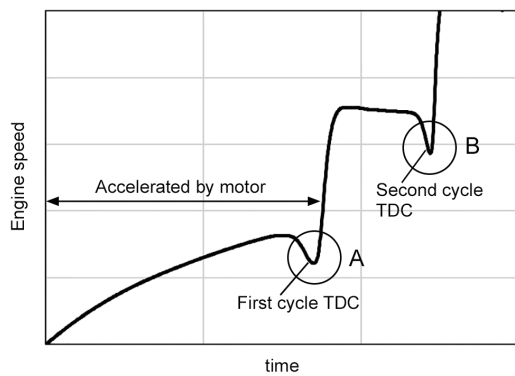


Fig.11 Fluctuation of engine speed at engine start

Based on the above, the calculation results for the startup time and instantaneous engine speed values when the decompressor timing (Fig. 12) is changed are shown in Figure 13. For the decompressor timing, the decompressor lift curve was kept constant with the reference to the crank angle for the base model, and only the decompressor activation angle was changed.

The operating conditions were warm-up restart for full throttle at an engine temperature of 60°C, and low-temperature startup at an engine temperature of -5°C.

Concerning about relation between decompression timing, starting time, and instantaneous engine speed, simulation results are shown in Figure 13.

Where, the value of the vertical axis is normalized with the engine starting time at the reference decompression timing.

The first graph in Figure 13 shows the decompressor timing advance is effective in reducing the startup time to reach idling speed in the warm-up restart.

The second graph shows however, too big advance of decompressor activation causes too low minimum engine speed during the first cycle, and results in failure of startup.

The third graph indicates that certain advance is necessary to avoid reoperation of decompressor during the second cycle.

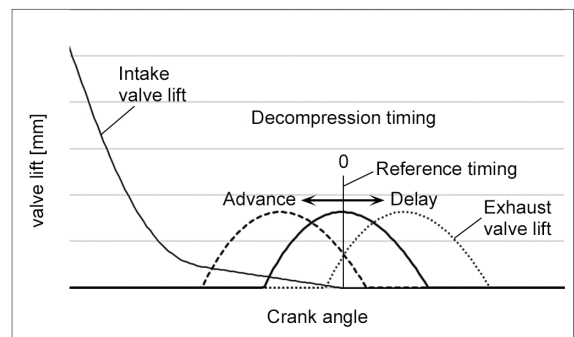


Fig.12 Timing of decompressor activation

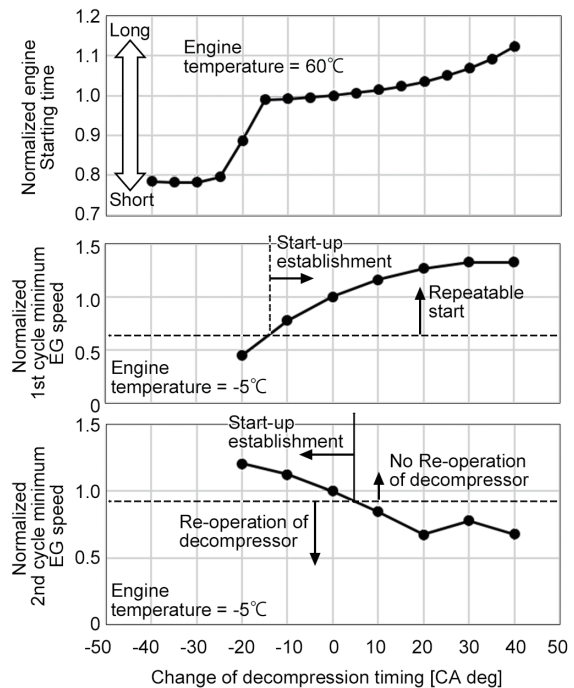


Fig.13 Relation between decompression timing, starting time, and instantaneous engine speed

By this, it was found that it is important for the engine speed to be within the possible ignition range and for the decompressor timing setting to be within the range capable of preventing decompressor reactivation in the second cycle. This simulation gives estimation of all these phenomena quantitatively. Thus, we have confirmed great potential of this simulation to determine the design specifications considering all these factors.

5 SUMMARY

1) It has been confirmed that the injection duration at startup is to be set so as to realize that the in-cylinder mixture is stoichiometry in order to both maximize the engine speed increase and minimize the fuel injection volume in the first combustion cycle at startup.

2) A fuel transport model capable of calculating the equivalence ratio in the cylinder has been proposed. This has been validated by comparing the results with experimental data.

3) A simulation incorporating such element as the fuel, motor, battery, and decompressor has been constructed. An example of investigation of starter motor control to satisfy the requirements for startability while considering air-fuel ratio control, has been presented.

4) Based on the above, the startup system simulation we have developed is expected to be quite effective in the process of startup system design.

REFERENCES

[1] Mizuoti, H., et al., "Development of "i-stop" (Mazda Idling Stop) System", JSAE Symposium Text 2010.2 34-38, 2010

[2] Ishizaki, K., et al., "Development of Technology for Engine Starting Vibration and Response", Proceedings of the Society of Automotive Engineers of Japan No.1-115, 444-448, 2016

[3] Sukegawa, Y., et al., "Study of Reduction Method of Hydro-carbon Emission during Cold-start for Direct

Injection Gasoline Engines", Proceedings of the Society of Automotive Engineers of Japan Vol.41, No.5, p.1037-1042, 2010

[4] Nakagawa, S., Ichihara, T., Katogi, K., Kanetoshi, K. et al., "An Air-Fuel Ratio and Ignition Timing Retard Control Using a Crank Angle Sensor for Reducing Cold Start HC", SAE Technical Paper, SAE-2008-01-1010, 2008

[5] Sakata, M., et al., "Simulation and Improvement of "i-stop" Engine Start Vibration", JSAE Symposium Text 2010.12 15-19, 2010

[6] Spalding, D.B., "The Combustion of Liquid Fuels", Fourth Symposium (International) on Combustion, Williams & Wilkins, Baltimore, 847-864, 1953

DEFINITIONS/ABBREVIATIONS

STD	standard
SMD	Sauter Mean Diameter
DC	Direct current
SOI	Start timing of Injection

■著者



伊東 善人
Yoshihito Ito
先進技術本部
研究開発統括部
基盤技術研究部



伊藤 大貴
Daiki Ito
先進技術本部
研究開発統括部
基盤技術研究部



飯田 実
Minoru Iida
先進技術本部
研究開発統括部
基盤技術研究部